Experimental Evaluation of Rock Erosion in Spillway Channels

George, M.F.
University of California, Berkeley, CA, USA

Sitar, N.
University of California, Berkeley, CA, USA

Sklar, L.
San Francisco State University, San Francisco, CA, USA

ABSTRACT: A series of flume experiments was performed as a part of a comprehensive study of rock erosion in spillway channels. The flume provided a controlled environment in which different flow rates and block configurations could be examined. The results of the experiments suggest that there is a strong influence of block orientation with respect to flow direction on the block erodibility threshold. Similarly, increasing flow turbulence intensity and/or increasing block protrusion height were also found to significantly lower the block erodibility threshold.

1. INTRODUCTION

Scour of rock occurs as a result of hydraulically driven removal of individual blocks (i.e., plucking or quarrying). This is a critical issue in many engineering projects, particularly for dams, bridges, and tunnels, where excessive erosion can threaten the stability of the structure. The same phenomenon accounts for geomorphic evolution of channels in hard, jointed rocks. Numerous investigations from both engineering and geomorphology perspectives have examined the erosion of rock blocks subject to a variety of flow conditions including open-channels [1 – 5], hydraulic jumps [6, 7], knick-points [8], and plunging jets/plunge pools [9 – 18]. A common focus has been the evaluation of the role of discontinuities bounding the block in transmitting hydraulic pressures to the underside of the block promoting ejection from the surrounding rock mass.

A lesser emphasis has been placed on the influence of the discontinuity orientations on kinematic modes of block removal. In nearly all studies, simplified rectangular or cubic block geometries were used with vertical and horizontal discontinuities thus limiting failure modes to predominantly 1D lifting or 1D sliding. For more complex block geometries, as commonly encountered in nature, the 3D orientations of the block bounding discontinuities strongly influence block removability, kinematics and stability [19]. Accordingly numerous kinematic failure modes exist. These include pure translational modes (lifting, 1-plane sliding, 2-plane sliding), pure rotational modes (about a corner, about an edge) or some combination of translational and rotational modes (Figure 1). The orientation of the block with respect to the direction of loading (e.g., flow direction) will determine the applicable mode of failure. From a scour perspective, this indicates the threshold for block erodibility (i.e., the flow condition causing removal of the block) will vary with the direction of the hydraulic forces.
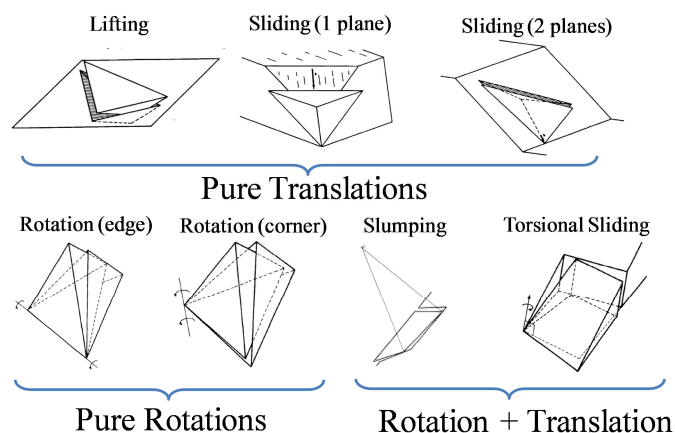

Fig. 1. Block kinematic failure modes [20].

Despite the importance of 3D geometry on erodibility, very little data exists, if any, regarding displacements and hydraulic pressures induced around 3D rock blocks. As such, a series of flume experiments with different flow rates and block configurations was carried out as

part of a comprehensive study of the hydraulics of 3D rock block erosion.

2. EXPERIMENTAL SETUP

Scaled physical hydraulic model tests were performed at the University of California's Richmond Field Station (RFS). Tests were conducted in a 28 m long x 0.85 m wide x 0.91 m deep flume with an overall grade of 1% (Figure 2). A wooden ramp was constructed within the flume to locally steepen the channel slope at the downstream end and increase flow velocity. The downstream section contained a rotatable block mold that housed a removable 3D tetrahedral rock block. The downstream channel grade was 20%, making an overall grade of 21% at the block location. This slope was constant for all tests.
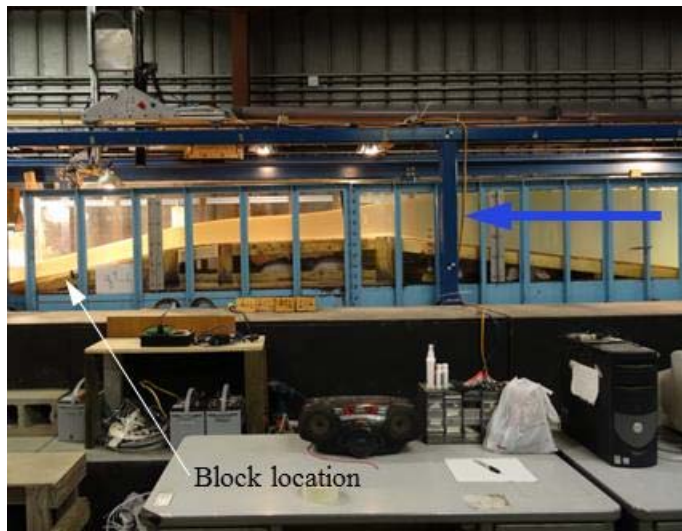

Fig. 2. Flume/ramp overview at RFS.

2.1. Block Mold
A 0.203 m (8") diameter plastic block mold was fabricated to house a 3D tetrahedral block and was installed flush with the channel bottom in the downstream section of the wooden ramp (Figure 3). The mold was constructed using 3D printing technology which provided considerable time and monetary savings (vs. manual fabrication) due to the numerous sensor slots that would have needed to be pre-drilled and the challenging angle cuts required between mold faces. One face of the mold was left open and fitted with clear acrylic plastic to provide viewing into the mold during testing.

The block mold could be rotated to change the orientation of the block with respect to the flow direction (Figure 3 – bottom). This was done in 15 deg. increments between 0 deg. and 180 deg.
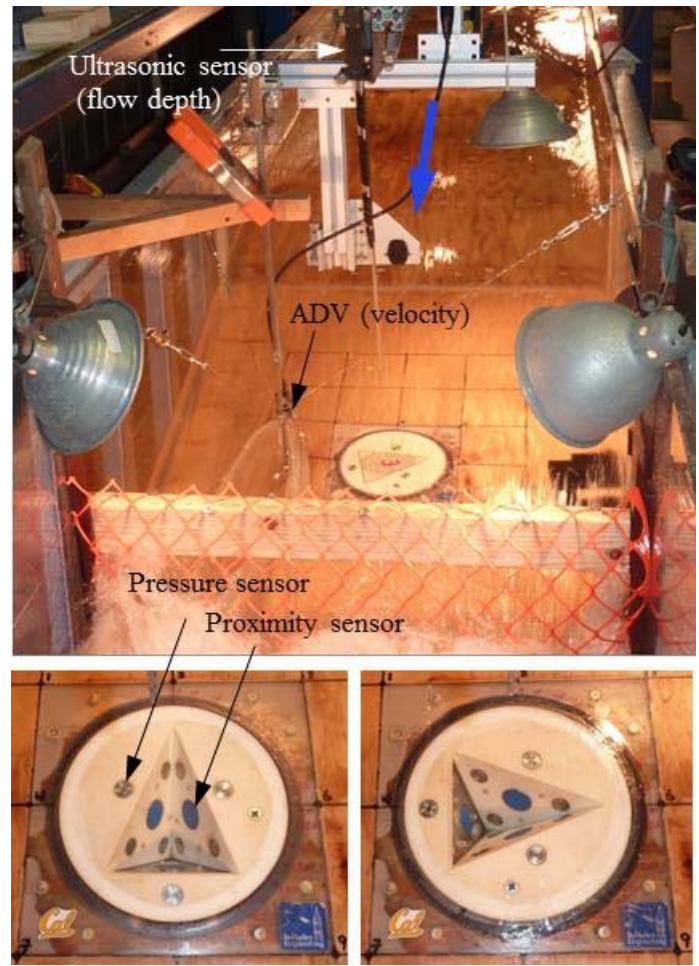

Fig. 3. Downstream ramp section showing block mold insert at angle of 75 deg. (top). Block mold at rotation angle = 0 deg. (bottom left) and rotation angle = 90 deg. (bottom right).

2.2. Blocks
Three tetrahedral shaped blocks were made with varying amount of protrusion height above the channel bottom (Table 1). Blocks were constructed from concrete and reinforced with fiberglass strands for added strength near block corners. Small, approximately 3 cm by 3 cm, stainless steel plates were added to the block faces directly opposite each proximity sensor (discussed below) for use as targets to determine discontinuity opening/block displacement.

Edges of the block protruding from the mold were rounded with a sander to more closely resemble a natural block edge in the field.

Table 1. Block Properties

Block #	1	2	3
Protrusion	4 mm	1.5 mm	Flush
Edge Type	Rounded	Rounded	Rounded
Weight	546.4 g	505.4 g	476.6 g
Volume	232 cm^3	224 cm^3	209.3 cm^3
Density	2.36 g/cm^3	2.26 g/cm^3	2.28 g/cm^3
Dimension 1	140.3 mm	138.7 mm	136.3 mm
Dimension 2	140.2 mm	138.9 mm	136.7 mm
Dimension 3	106.6 mm	103.7 mm	104.6 mm
Dimension 4	106.7 mm	104.4 mm	103.3 mm
Dimension 5	107.5 mm	104.0 mm	104.2 mm
Dimension 6	131.2 mm	130.0 mm	127.0 mm
Notes: Schematic for block dimensions			

2.3. Instrumentation/Data Acquisition

The flume channel and block mold were instrumented with sensors to characterize flow conditions in the vicinity of the block as well as to record block displacements and measure dynamic pressures within the discontinuities bounding the block. The following is a list of sensors and data acquisition tools used:

- Pressure – Keller PR-9FLY & PR-23Y, 0-0.5 bar, 0-5 VDC output, vented gauge pressure transmitters. Three sensors per block mold face and three sensors flush with channel bottom near center of discontinuity openings (Figure 2). Smaller PR-23Y model sensors were used on the clear acrylic face due to space limitations. Sampling frequency = 100 Hz.

- Displacement – SICK IMA30-20BE1ZCOK, 0-20mm range, 4-20 mA output, inductive analog proximity sensors. One sensor per block mold face. A stainless steel target was installed directly opposite each sensor on the block. Sampling Frequency = 100 Hz.

- Flow Depth – Massa M-5000, 0.1-1.0 m range, 8 deg. conical beam, ultrasonic sensor. Sensor installed directly above block mold, perpendicular to channel slope. Sampling Frequency = 50 Hz with boxcar averaging every 100 samples.

- Flow Velocity – 1) Nortek side-facing Vectrino acoustic Doppler velocimeter (ADV) with Plus firmward upgrade. Sampling Frequency = 100 Hz during runs with pressure and displacement measurements and 200 Hz during runs for flow characterization. 2) 0.3175 cm (1/8") OD acrylic pitot tube located at channel bed.

- Data Acquisition – 1) Campbell Scientific CR-3000 datalogger for pressure and displacement measurements. 2) Toshiba Portege R705 laptop PC for ADV and flow depth measurements. ADV was synchronized with pressure and displacement measurements using a pulse trigger mechanism from the CR-3000.

2.4. Testing Strategy

Several test configurations were used to characterize the block response to channel flows. Four main variables were monitored within the realm of this study. These included:

- Block orientation – Block orientation with respect to flow direction was varied by rotating the block mold in 15 deg. increments between 0 – 180 deg. It was not necessary to do a full 360 deg. rotation due to block symmetry.

- Block Protrusion – Three block protrusion heights of 0 mm (flush), 1.5 mm and 4.0 mm were examined.

- Turbulence Intensity – Low and high turbulence cases were studied. Turbulence was generated with the addition of seven staggered baffles upstream of the block. Degree of turbulence was quantified using turbulence intensity (Tu) which relates the root mean square (RMS) of the vertical velocity component, v'_z, to the mean horizontal flow velocity component, v_x.

- Flow Velocity – Nine flow velocities, corresponding to nine different flow rates, Q1 – Q9, were used. To generate the different flow rates, three pumps were used with a maximum capacity of 0.3 m^3/s (0.1 m^3/s each). A variable speed controller was used with one of the pumps such that any flow rate between 0-0.3 m^3/s could be achieved.

In general, two types of tests were conducted. One was to determine the block erodibility threshold. For these tests, the discharge was increased incrementally (from Q1 to Q9) for periods of approximately 5 minutes until the block failed. If block displacements appeared to be continually increasing, the run length was extended. The other type was to determine statistical distributions of the dynamic pressures on the block faces. Four flow rates (Q1, Q3, Q6 and Q9) were tested. If a block had previously failed at a lower flow rate, a rod was placed on top of the block to hold the block in place such that high flow rates could be realized.

3. RESULTS

3.1. Flow Characterization

General flow characteristics in the vicinity of the block for the nine flow rates are provided in Table 2. ADV time series data was filtered using a phase-space despiking algorithm developed by [21], modified by [22] and included as part of the WinADV processing software [23]. Mean horizontal velocity, v_x, values and RMS vertical velocity values, v'_z, were extracted to calculate turbulence intensity (Tu). Note that Tu values for discharges Q1-Q3 could not be determined as the entire ADV was not submerged and the vertical velocity component could not be reliably measured. It is anticipated, however, Tu values for those flows would likely be comparable to those for the other discharges.

Table 1. Flow properties at block location

Flow	Low Tu		High Tu	
	v_x (m/s)	Tu (%)	v_x (m/s)	Tu (%)
Q1	2.33 (7.38)	-	2.08 (6.59)	-
Q2	2.44 (7.70)	-	2.10 (6.65)	-
Q3	2.51 (7.93)	-	2.22 (7.00)	-
Q4	2.64 (8.35)	2.78%	2.38 (7.52)	6.61%
Q5	2.71 (8.58)	2.48%	2.55 (8.07)	5.98%
Q6	2.76 (8.72)	2.46%	2.59 (8.19)	6.25%
Q7	2.84 (8.97)	2.21%	2.67 (8.45)	6.13%
Q8	2.92 (9.23)	2.15%	2.70 (8.54)	6.95%
Q9	2.96 (9.35)	2.17%	2.71 (8.57)	7.39%
Notes: v_x values in parenthesis are prototype scale velocity values determined using a model/prototype length scale ratio of 1/10 (Froude scaling).				

3.2. Block Erodibility Threshold

Results for block erodibility threshold for Block 2 (protrusion height = 1.5 mm) are presented in Figure 4 for both the high and low turbulence intensity cases. Critical velocity values provided are prototype scale. A range of values are provided (indicated by a line connecting two bounding data points) when failure of the block occurred between two flow rates (i.e., while flow was ramping up from previous to next discharge).
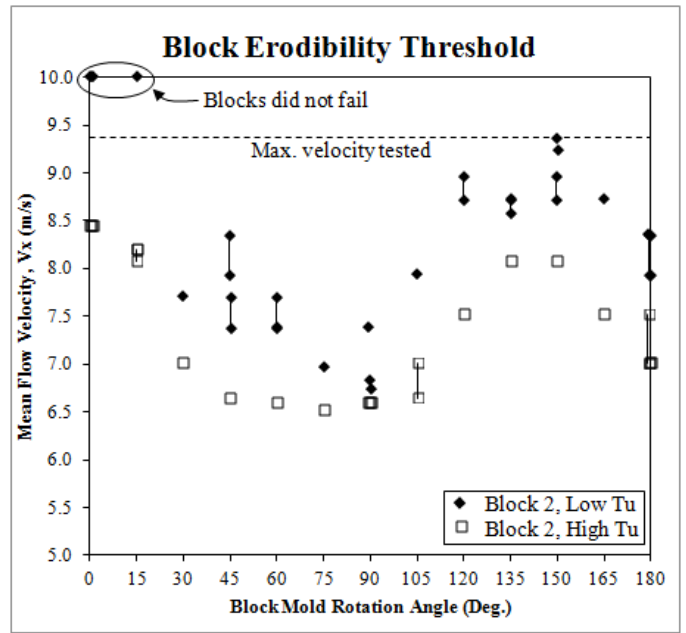

Fig. 4. Block 2 erodibility threshold as a function of block orientation with respect to flow direction, high and low Tu scenarios.

As indicated, the threshold condition for incipient motion of the block is highly dependent on the orientation of the block with respect to the flow direction. For the low Tu scenario, Block 2 could not be eroded under any discharge when the rotation angle of the block mold was 0 and 15 deg. (see Figure 2). This configuration corresponds to a geometry where the downstream face of the block mold is fairly steep making removal of the block kinematically more difficult. Additionally, the block profile protruding into the flow is narrow resulting in a minimal drag force applied to the block. This is opposed a block with a very wide profile, corresponding to a block mold rotation of 60-90 deg., where the drag force is maximum. Additionally, the intersection of the two downstream block mold faces provides a shallower sliding path for the block, making it kinematically easier to remove. As such, the block erodibility threshold in these locations is a minimum.

The influence of increased turbulence, as observed in the High Tu data set in Figure 4, decreases the block erodibility threshold fairly evenly across the range of block orientations. In general for this particular block type, a 2-3% increase in turbulence intensity results in approximately a 10% decrease in the mean flow velocity required to remove the block. This is a particularly important result as it suggests that velocity alone is poor indicator of incipient motion (this is discussed further below).

The influence of block protrusion height can be seen in Figure 5 which compares block erodibility threshold for Block 2 (protrusion height = 1.5 mm) versus Block 1 (protrusion height = 4 mm) as a function of block mold rotation angle.
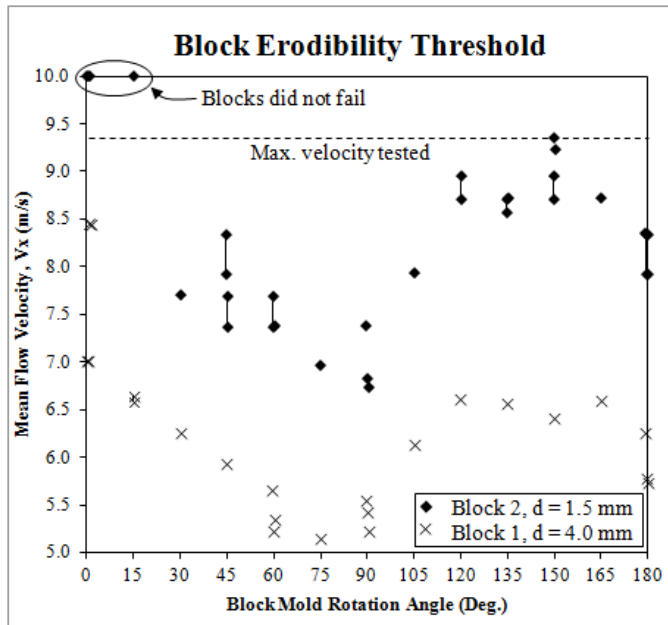

Fig. 5. Block erodibility threshold as a function of block orientation with respect to flow direction for Block 1 (protrusion, d = 4.0 mm) and Block 2 (protrusion, d = 1.5 mm), low Tu scenario.

As indicated, a higher block protrusion height results in a lower block erodibility threshold. This outcome is anticipated due to the increased drag force associated with the block becoming more exposed in the flow. This agrees with other testing performed by the United States Bureau of Reclamation for hydraulic jacking of concrete slabs in spillway channels [3]. Similar to the case for increased turbulence intensity, increased block protrusion appears to result in a nearly uniform reduction in critical mean velocity across the range of block orientations.

For a block flush with the surrounding channel bottom (Block 3) with similar joint openings to the other two blocks, no removal occurred under any tested flow conditions.

4. CONCLUSIONS

Scaled physical hydraulic model tests were performed to fully characterize behavior of a 3D tetrahedral rock block subject to channel flow conditions. The results show that the block erodibility threshold is strongly dependent on the orientation of the block with respect to the flow direction. This result is namely related to two

factors: 1) change in the dominant kinematic constraints resulting from changes in orientation of the applied load, and 2) changes in the block profile in the flow. The former influences the ease at which the block may be removed from its mold, while the latter influences the relative magnitude of the surficial drag force applied to the block.

The experiments with varying degrees of turbulence intensity showed that a block may be eroded at a relatively low mean flow velocity provided the flow also has a higher degree of turbulent fluctuations. This is a particularly important result in the sense that velocity alone would not be a particularly good indicator parameter of erosion threshold. Consider, for example, a scenario of water flowing over a smooth surface. As the material begins to erode, the surface becomes rough and the flow velocity slows down. Purely considering velocity as an indicator would lead to the conclusion that erosion would also decrease. The results herein suggest, however, that although the mean flow velocity would decrease the turbulence generated due to roughening of the surface would act to actually increase erosion. Accordingly, assessment of flow erosive capacity should address both flow velocity and degree of turbulence.

5. ACKNOWLEDGEMENTS

REFERENCES

1. Reinius. 1986. Rock erosion. *Water Power and Dam Construction*, June, 43-48.

2. Coleman, S.E., Melville, B.W., and L. Gore. 2003. Fluvial entrainment of protruding fractured rock. *J. of Hyd. Eng*. 129(11): 872-884.

3. USBR (2007). Uplift and crack flow resulting from high velocity discharges over open offset joints. *Report DSO-07-07*, United States Bureau of Reclamation, Denver.

4. Dubinski, I.M. 2009. Physical modeling of jointed bedrock erosion by block quarrying. *PhD Disseration*. Colorado State University.

5. Chatanantavet, P. and G. Parker. 2009. Physically based modeling of bedrock incision by abrasion,

plucking, and macroabrasion. *J. of Geophys. Research* 114 F04018.

6. Fiorotto, V. and Rinaldo, A. 1992. Fluctuating uplift and lining design in spillway stilling basins. *J. of Hyd. Eng.*, 118(4): 578-596.

7. Fiorotto, V. and P. Salandin. 2000. Design of anchored slabs in spillway stilling basins. *J. of Hyd. Eng.*, 126(4): 502-512.

8. Lamb, M.P. and W.E. Dietrich. 2009. The persistence of waterfalls in fractured rock. *GSA Bulletin*. 121(7/8): 1123-1134.

9. Yuditskii, G.A. 1967. Actual pressure on the channel bottom below ski-jump spillways. *Izvestiya Vsesoyuznogo Nauchno-Issledovatel-Skogo Instuta Gidrotekhiki*, 67: 231-240 (in Russian).

10. Annandale, G.W. 1995. Erodibility. *J. of Hyd. Research*. 33: 471-494.

11. Annandale, G.W. 2006. *Scour Technology*. 1st ed. New York: McGraw-Hill.

12. Liu. P., Dong, J. and C. Yu. 1998. Fluctuating uplift on rock blocks at the bottom of a scour pool by overfall jets. *Science in China (Series E)*. 41(2): 130-139.

13. Robinson, K.M., and K.C. Kadavy. 2001. Pressure forces in a fractured matrix. *Proc. of the ASAE Int. Meeting*, Sacramento, CA USA.

14. Bollaert, E. 2002. Transient water pressures in joints and formation of rock scour due to high-velocity jet impact, *Communication No. 13*. Laboratory of Hydr. Constructions, Ecole Polytechnique Federale de Lausanne, Switzerland.

15. Manso, P. 2006. The influence of pool geometry and induced flow patterns in rock scour by high-velocity plunging jets, *Communication No. 25*, Laboratory of Hydraulic Constructions, Laboratory of Hydr. Constructions, Ecole Polytechnique Federale de Lausanne, Switzerland.

16. Melo, J.F., A.N. Pinheiro, and C.M. Ramos. 2006. Forces on plunge pool slabs: influence of joints location and width, *J. of Hyd. Eng.*, 132(1): 49-60.

17. Federspiel, M., Bollaert, E., and A. Schleiss. 2011. Dynamic response of a rock block in a plunge pool due to asymmetrical impact of a high-velocity jet. *Proc. from the 34rd IAHR Congress*, Brisbane, Australia.

18. Duarte, R.X.M. 2014. Influence of air entrainment on rock scour development and block stability in plunge pools, *Communication No. 59*, Laboratory of Hydraulic Constructions, Laboratory of Hydr. Constructions, Ecole Polytechnique Federale de Lausanne, Switzerland.

19. Goodman, R.E. and G. Shi. 1985. *Block Theory and Its Application to Rock Engineering*. Englewood Cliffs, N.J.: Prentice Hall.

20. Goodman, R.E. 1995. Block theory and its application. *Geotechnique* 45(3): 383-423.

21. Goring, D. and Nikora, V. 2002. Despiking acoustic doppler velocimeter Data. *J. of Hyd. Eng.*, 128(1): 117-126.

22. Wahl, T. L. 2003. Discussion of "Despiking Acoustic Doppler Velocimeter Data". *J. of Hyd. Eng*, 129(6).

23. Wahl, T. L. 2000. Analyzing ADV data using WinADV. *Proc. of Joint Conference on Water Resources Engineering and Water Resources Planning and Management*, American Society of Civil Engineers, July 30–August 2, Minneapolis www.usbr.gov/wrrl/twahl/winadv.